NRIAG Journal of Astronomy and Geophysics 6 (2017) 256–266

Contents lists available at ScienceDirect

NRIAG Journal of Astronomy and Geophysics

journal homepage: www.elsevier.com/locate/nrjag

Case report

Joint application of Geoelectrical Resistivity and Ground Penetrating Radar techniques for the study of hyper-saturated zones. Case study in Egypt

Hany S. Mesbah [a,*], Essam A. Morsy [b], Mamdouh M. Soliman [a], Khamis Kabeel [a]

[a] National Research Institute of Astronomy and Geophysics
[b] Geophysics Department, Faculty of Science, Cairo University

ARTICLE INFO

Article history:
Received 21 September 2016
Revised 25 February 2017
Accepted 6 April 2017
Available online 27 April 2017

Keywords:
Geoelectrical Resistivity Sounding
Ground Penetrating Radar GPR
Joint application
Hyper saturated zones
Qualitative and quantitative interpretation

ABSTRACT

This paper presents the results of the application of the Geoelectrical Resistivity Sounding (GRS) and Ground Penetrating Radar (GPR) for outlining and investigating of surface springing out (flow) of groundwater to the base of an service building site, and determining the reason(s) for the zone of maximum degree of saturation; in addition to provide stratigraphic information for this site. The studied economic building is constructed lower than the ground surface by about 7 m. A Vertical Electrical Sounding (VES) survey was performed at 12 points around the studied building in order to investigate the vertical and lateral extent of the subsurface sequence, three VES's were conducted at each side of the building at discrete distances. And a total of 9 GPR profiles with 100- and 200-MHz antennae were conducted, with the objective of evaluating the depth and the degree of saturation of the subsurface layers. The qualitative and quantitative interpretation of the acquired VES's showed easily the levels of saturations close to and around the studied building. From the interpretation of GPR profiles, it was possible to locate and determine the saturated layers. The radar signals are penetrated and enabled the identification of the subsurface reflectors. The results of GPR and VES showed a good agreement and the integrated interpretations were supported by local geology. Finally, the new constructed geoelectrical resistivity cross-sections (in contoured-form), are easily clarifying the direction of groundwater flow toward the studied building.

1. Introduction

Problems of groundwater and the hydrological systems of particular sites are commonly investigated with vertical electrical sounding and Ground Penetrating Radar (GPR) techniques. The conventional approach of drilling requires use of both a water boring contractor and a geologist on-site for several days, and is quite expensive. Correctly applied geophysics will reduce the number of drill-holes required to attain detailed information on the hydrological and geological system (Humphreys et al., 1990).

The scientific literature includes many examples of the successful use of the geoelectrical methods in the study of groundwater problems (e.g., Swartz, 1937; Tellam et al., 1985). The nondestructive nature of the Ground Penetrating Radar (GPR) tool is of interest for a variety of engineering and environmental applications (Stockbauer and Kalinec, 1995).

The problem of over-saturation and springing-out of groundwater around the touristic building is considered one of the main concerns of earth scientists and researchers in Egypt due to rising of groundwater levels in/around archaeological sites. Our problem was formulated by, the base of service building of hotel in 6th of October City were intervened by infiltrated groundwater (Fig. 3). Moreover, All the domestic, drinking water and sanitary buried pipelines leading to and around the service building were investigated enough to determine if there is any type of corrosion, which is confirmed by, there is no any disconnection and leakage for these pipelines.

In such context, the integrated use of geophysical methods provides an important tool in the characterization of the reasons

* Corresponding author.
E-mail address: hmesbah2000@yahoo.com (H.S. Mesbah).
Peer review under responsibility of National Research Institute of Astronomy and Geophysics.

Production and hosting by Elsevier

http://dx.doi.org/10.1016/j.nrjag.2017.04.002

of groundwater flow through the building and percolation of the infiltrated groundwater toward the studied site and/around of the building.

2. Local geology

The 6th of October City is one of the new cities in Egypt, southwest of Greater Cairo area (Fig. 1) with 160–200 m above sea level. The geological studies of 6th of October City show that, several times by the sea "Tethys". This old geologic sea probably began to form in the pre-Cambrian era and is considered the antecedent of the Mediterranean Sea. It has always encroached upon the land of Egypt from the north. This means that Egypt's past land - sea distribution has not always been the same as it is today. The proof is the great quantity of sea shells spread over the surface of the City (Saad et al., 2015).

Ground material is formed mainly of yellowish to reddish brown calcareous slightly cemented sand. The observed binding materials are carbonates, iron oxides, sometimes salt and gypsum. Unconformities in these formations between many stages and of all magnitudes are found. This could be due to the turbulence in the sedimentation process according to the varying movement of water courses (Saad et al., 2015). Fig. 2 shows the different sedimentation in the vicinity of the city that leads to the great difference in the soil distribution within the city. In general, the surface sediments in the studied area are loose to very loose mixture of sand, gravel silt, and shale deposits (Fig. 4).

3. Data acquisition

3.1. Electrical resistivity data

A total of 12 VES stations were measured (Fig. 5) using SYSCAL-R2 instrument, and Schlumberger array was applied with maximum current electrode spacing of AB/2 = 200 m. The electrode spread was along the available space along sides of the building, the data were acquired with a degree of accuracy of six points per decade, and the number of stacks of 10 times to achieve the maximum resolution. VES data were interpreted using a 1D forward and inverse modeling program "RESIST" software. Local geology, shallow boreholes were used to calibrate the thickness of the geoelectrical layers used in the inversion process.

3.2. GPR data

Fig. 5 also shows the location of the acquired 9 GPR profiles. The survey was carried out using Mala Geoscience (Ramac-GPR) equipment with 100- and 200-MHz unshielded antennae. Georadar data were collected with a 1-m antenna gap (for the 100 MHz) and 0.6 m (for the 200 MHz) with 36 stacking for each trace. The triggering factor was based on time and 512 vertical stacks, and the transmitting and receiving antennae were positioned in transversal orientation to the profile direction in order to guarantee maximum coupling between the transmitted and the received signals (Annan, 1992; Annan and Cosway, 2002; Versteeg, 1996).

Impulse radar techniques are based on the propagation of short electromagnetic pulse, which transmitted through pavement and then partly reflected from electrical interfaces within the subsurface geologic sequence. Electrical interfaces occur when the GPR wave encounters different materials or changes in either moisture content or density. The surveyed profiles are presented as a function of both time and depth. The time/depth conversion is based on a standard velocity value of 0.07 m/ns, compatible with a saturated clay deposits (Davis and Annan, 1989; Annan, 1992). The data is processed using the traditional filters to recover the energy lost through absorption due to saturation of subsurface materials, such as, linear and exponential gain and depth conversion using the velocity of 0.07 m/ns, also a three scan moving average filter was applied to the data and resulted in horizontal smoothing.

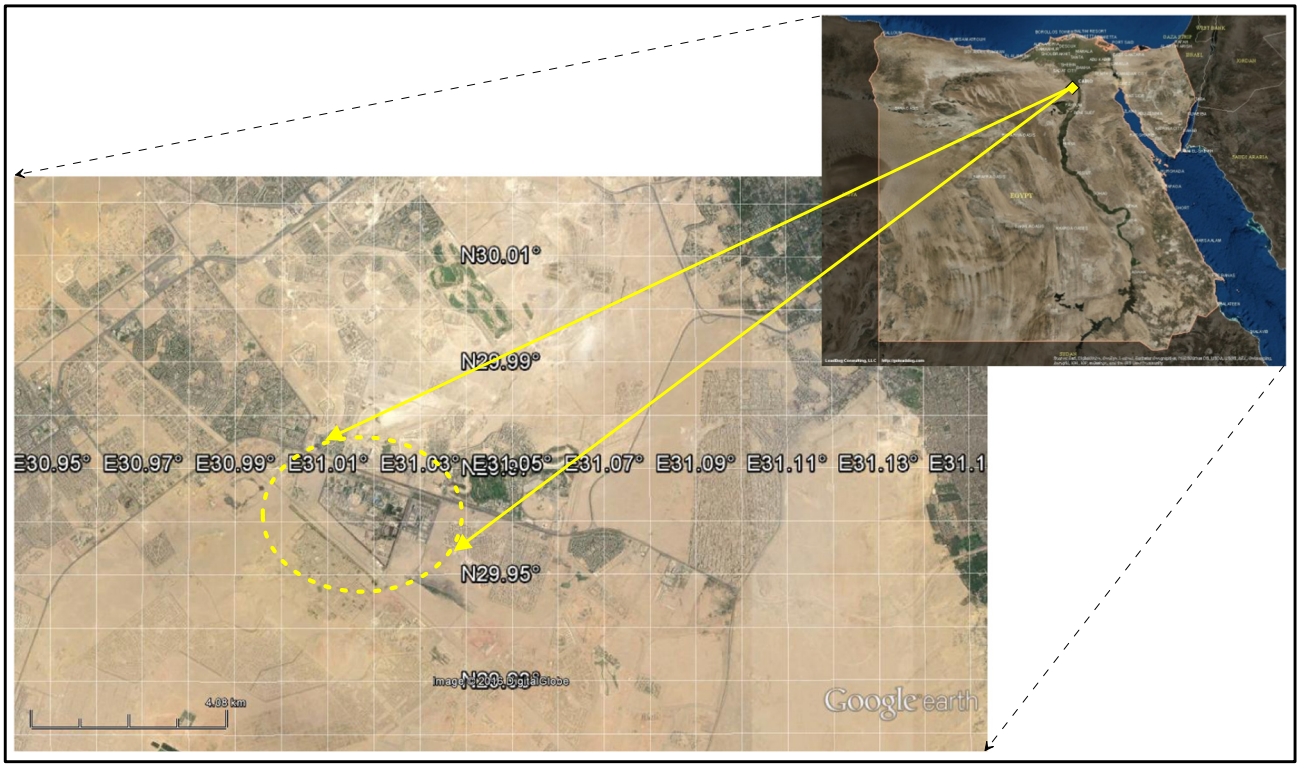

Fig. 1. Location map of the study area.

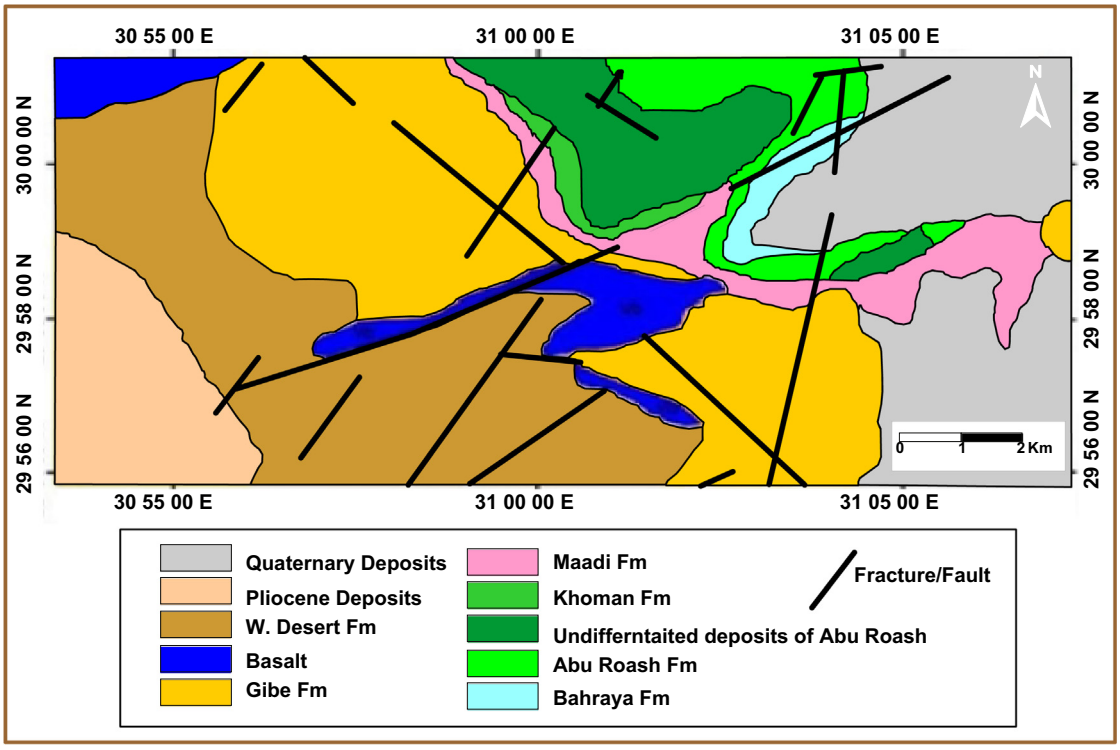

Fig. 2. Geological map of 6th October City (after Conco Coral, 1987).

Fig. 3. Panoramic view showing the studied site.

4. Interpretation and results

4.1. Electrical resistivity data

The geoelectric resistivity data are interpreted quantitatively and qualitatively as well as ground penetrating radar data.

The approach utilized in the interpretation of the available VES's of the study area, as acquired through Schlumberger configuration, depend on a number of steps arranged sequentially. First, the electrical noises superimposed on the field curve are removed using an adequate filter operator to leave this curve in a smoothed form, as shown by Ghosh (1971), Secondly, the process of matching

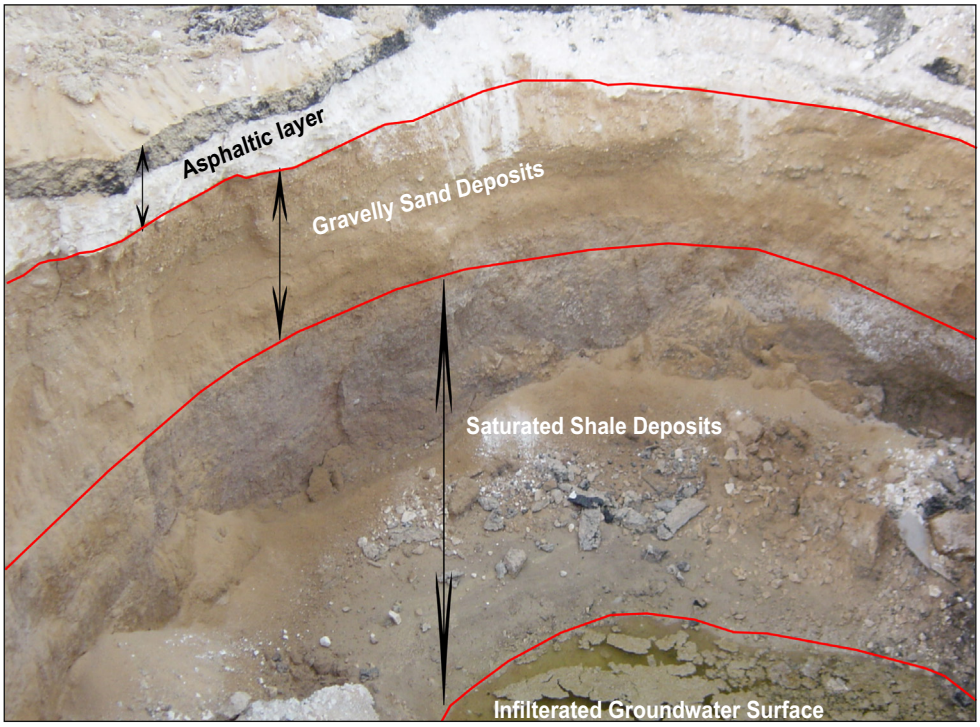

Fig. 4. A small borehole showing the shallow subsurface layers.

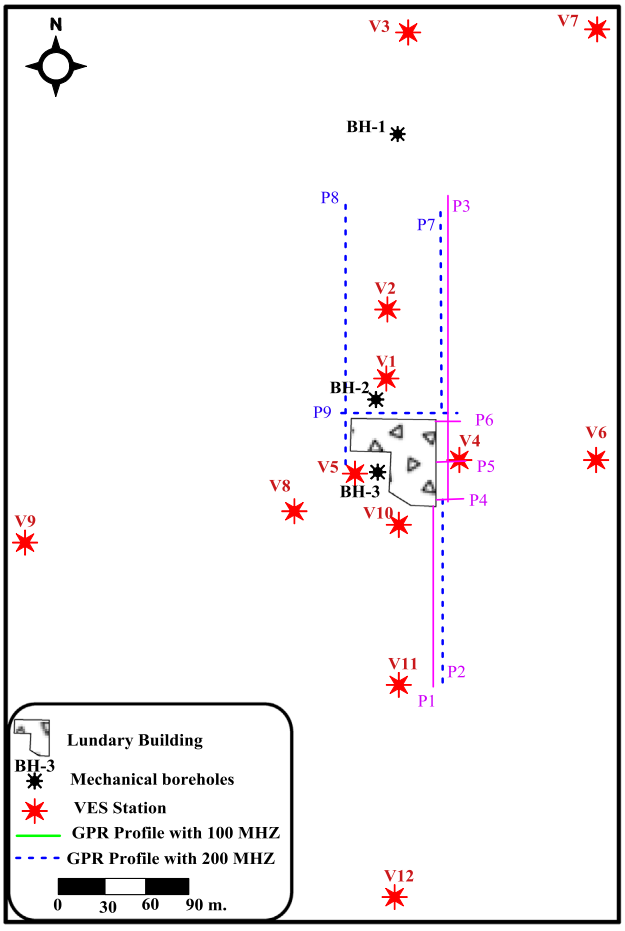

Fig. 5. Schematic map of the survey site showing mechanical boreholes, VES locations, and GPR profiles around the Laundry building.

the smoothed field curve with the standard curves of the auxiliary method is based on a higher degree of fitting regarding the curve parameters, as illustrated by Marsden (1973) and Mooney et al. (1966). Thirdly, the process of defining the depths of the existing boundaries between each two consecutive beds and the repetition of this operation for a limited number of layers, as explained by Patella (1975). Fourthly, the carrying out the afore-mentioned steps by a computer interpretation package is performed, as expressed by Johansen (1977). Finally, the extension of this analytic technique for any number of layers constituting the evaluated section (N-layers) is accomplished through the accumulation of the layers, as explained by Szaraniec (1979).

Consequently, the acquired VESes at the study area are analyzed in terms of layers is done of certain actual resistivities and well defined depths for the upper and lower surfaces of the encountered beds. Figs. 6 and 7 represents four samples of the conducted VES's and their resultant geoelectric models.

To demonstrate the distribution of the calculated resistivity parameters (true resistivity and thickness) in the vertical planes across the studied area, four cross sections are constructed. The geoelectric cross sections revealed a general subsurface resistivity model consisting of four main resistivity layers (Figs. 8 and 9):

(1) A surface resistivity layer having a variable resistivity range of 3.4–278.4 Ω m corresponding to surface and asphaltic materials. The average thickness of this layer reaches about 2 m.
(2) The second resistivity layer having a resistivity range of 8.5–41.4 Ω m corresponding to partially saturated gravely sand and sand deposits. The thickness of this layer varies between 1.7 and 5.3 m.
(3) The third resistivity layer having a resistivity range of 1.2–21.7 Ω m corresponding to the saturated shale deposits. The thickness of this layer varies between 9.8 and 30.8 m.
(4) The bottom layer corresponds to partially saturated shale with a resistivity ranging between 6.6 and 30.5 Ω m.

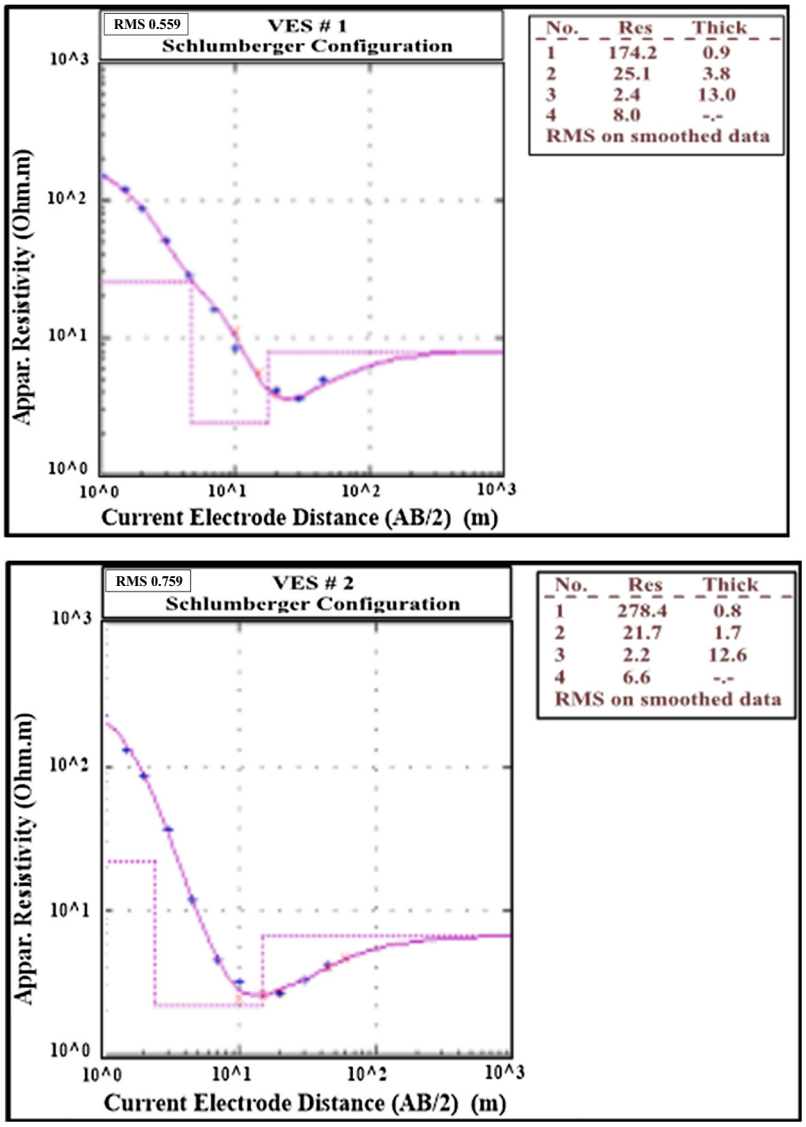

Fig. 6. Samples of geoelectric resistivity models of VES's 1 and 2.

Utilizing the results of the resistivity modeling procedure, a set of contour maps and a number of cross-sections are constructed, respectively, to illustrate the lateral and vertical distributions of the calculated resistivity parameters (i.e., true resistivity and thickness) throughout the study area.

Fig. 10 shows the areal distribution of the true resistivity of the third saturated layer throughout the studied site, which showing the true resistivity was about of 2.0 Ω m and reaches to about 20.0 Ω m around the boundary of the studied site. From the physical definition of resistivity and its direct relationship to water content, the true resistivity is dependent mainly on the degree of saturation, so the values of the true resistivity along and around the studied site is decreased as a result of increasing of water content and clay content along and around the building.

Electrical resistivity, which is the inverse of electrical conductivity, is a fundamental property that varies in the earth with rock or sediment type, porosity, and the quality and quantity of water. Generally, electricity is conducted in the earth electrolytically by interstitial fluids (usually water) and electronically by certain materials (such as clay minerals). Because of this, saturated layers with high clay content have lower resistivity (Jared and Jeffrey, 2004).

The traditional constructed geoelectric resistivity cross-sections (Figs. 8 and 9) are not able to illustrate the lateral distributions of the calculated resistivity parameters, So, it was efficient and of valuable representation to clarify these geoelectric resistivity cross-sections in a contoured form than conventional pseudo-sections for showing the degree of saturations of the different subsurface layers and the direction of flow of infiltrated water through the subsurface layers.

Fig. 11a–d shows the geoelectric resistivity cross-section-contoured-form, which clarify easily the direction of decreasing true resistivity toward the laundry building, i.e., direction of increasing degree of saturations that was directly related to the direction of flow of infiltrated water through the shallow subsurface layer.

4.2. GPR profiles

Interpretation procedures followed in interpreting the present GPR data are adopted in part from many of papers and workshop reports. The following is a brief description of the conducted GPR profiles:

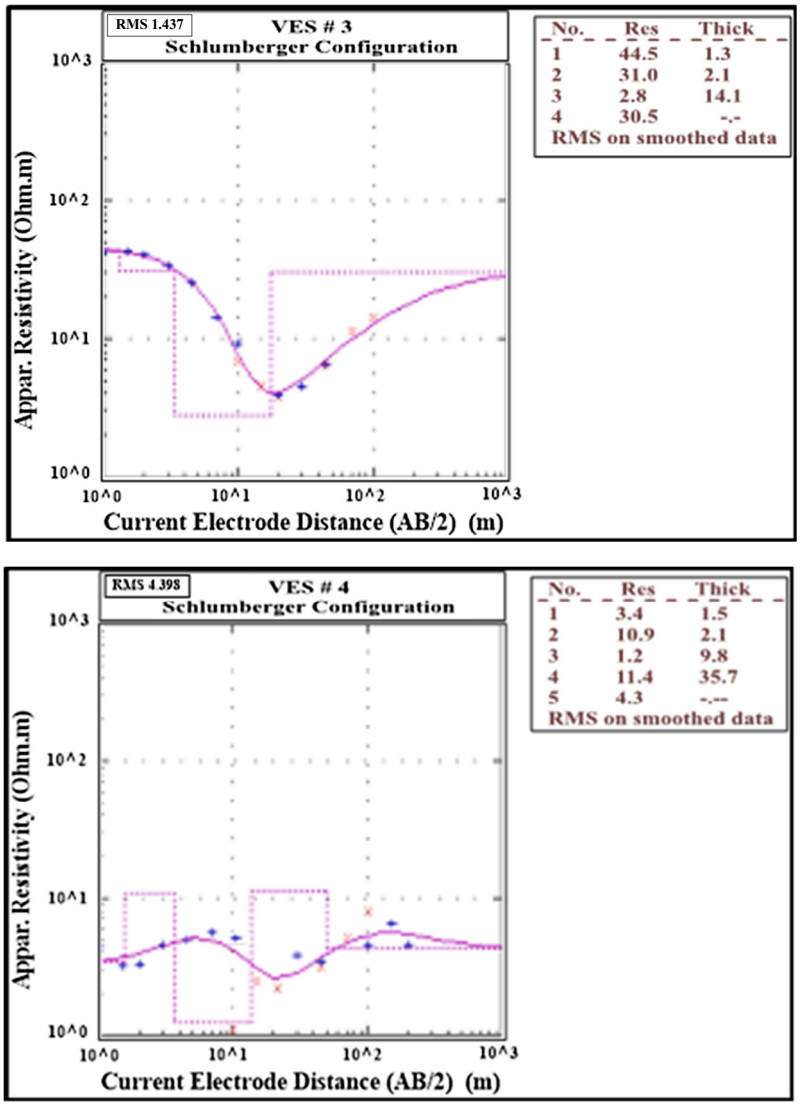

Fig. 7. Samples of geoelectric resistivity models of VES's 3 and 4.

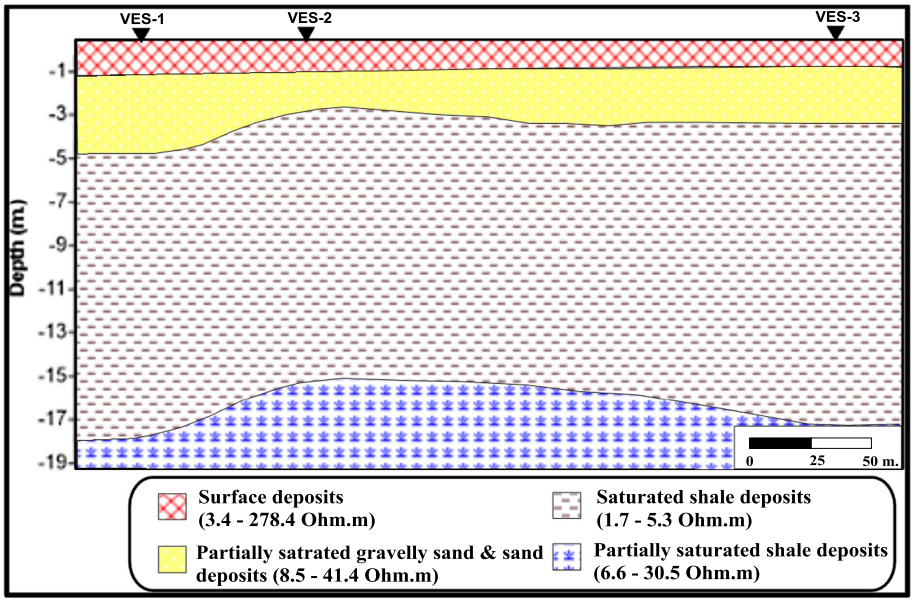

Fig. 8. Geoelectric resistivity cross-section P#1.

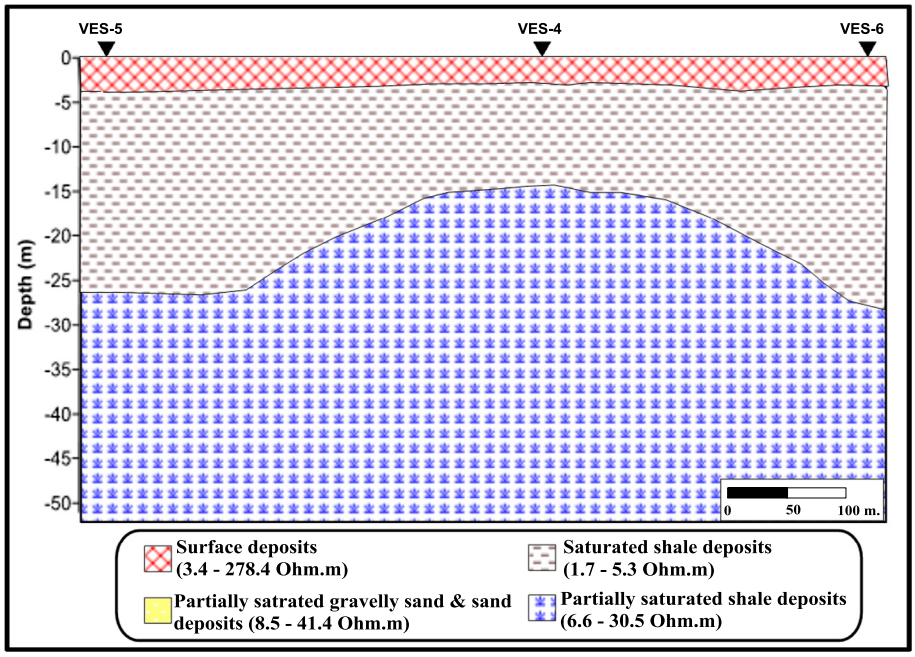

Fig. 9. Geoelectric resistivity cross-section P#2.

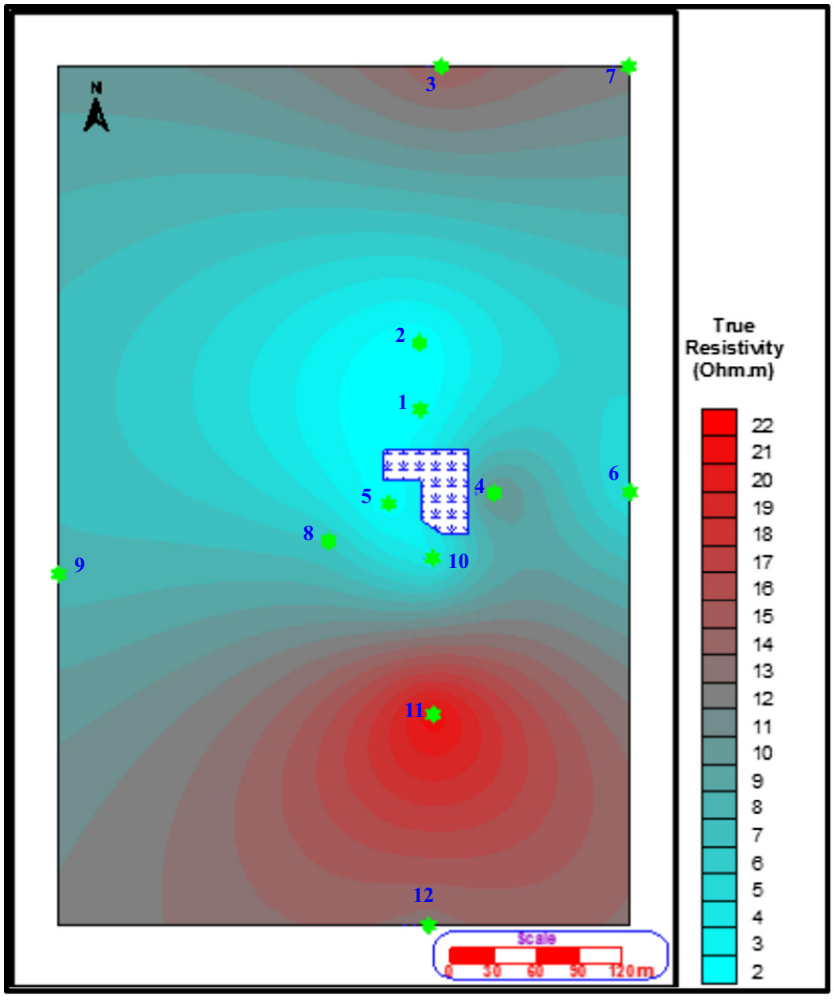

Fig. 10. True Resistivity contour map of the saturated third layer through the study area.

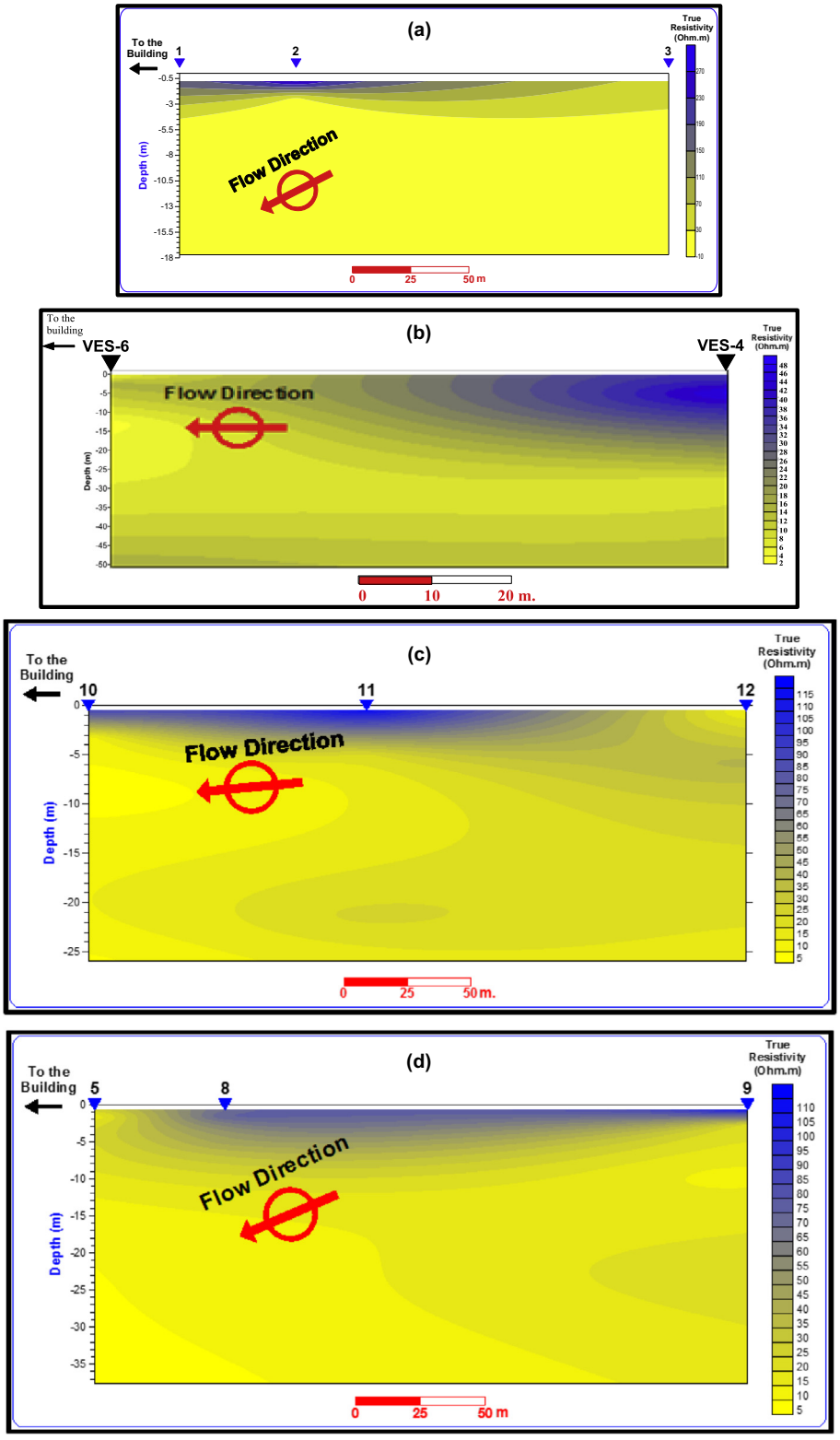

Fig. 11. (a) Geoelectric resistivity cross-section. (b) Geoelectric resistivity cross-section. (c) Geoelectric resistivity cross-section. (d) Geoelectric resistivity cross-section.

- GPR Profile 1:

This Profile was conducted on the southern part of the building, from the south to the north with 130 m length (Fig. 5), by the 100 MHz antenna (Time Window ***TW*** = 420 ns) and applying the velocity of soil of 0.07 m/ns (the maximum depth of penetration is about 16 m). The profile (Fig. 12) reveals that, there are four distinctive layers, (1) the first layer of a thickness of about 0.8 m which corresponds to the surface exposed layer that consists of paving and weathered materials, (2) a second layer of 2 m thickness corresponds to saturated sandy shale deposits, (3) third layer represented on the section by a strong reflector that corresponds to

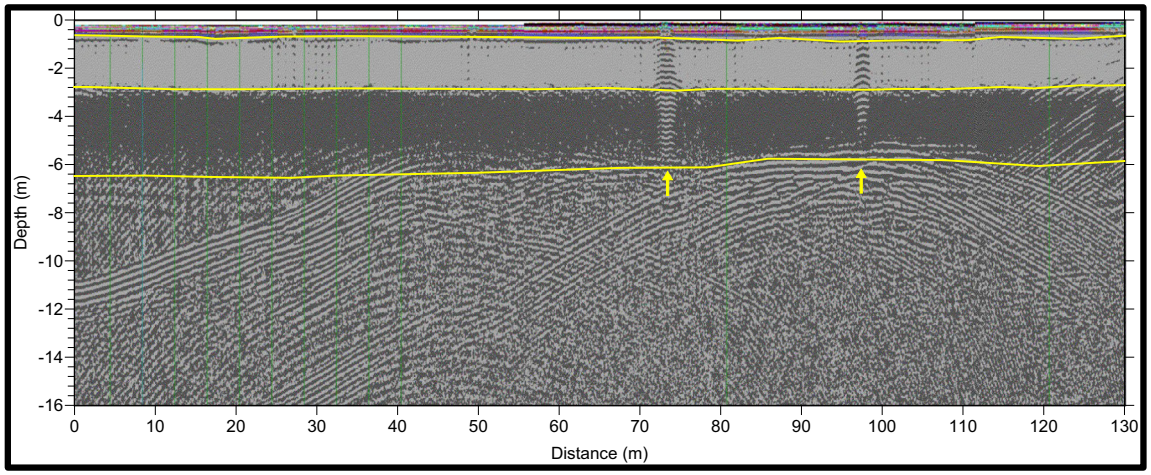

Fig. 12. GPR profile #1 (100 MHz antenna). (The yellow arrows refer to utilities on the studied site).

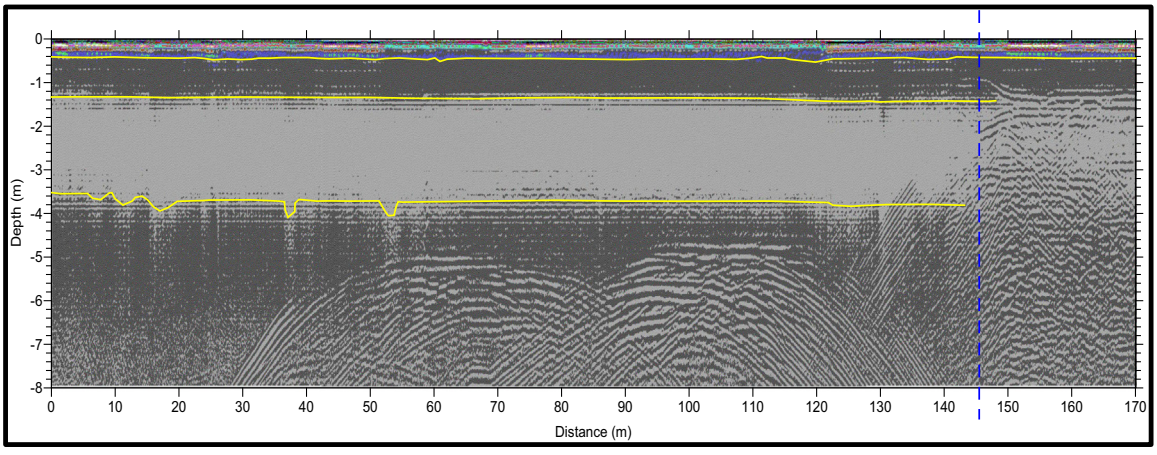

(a)

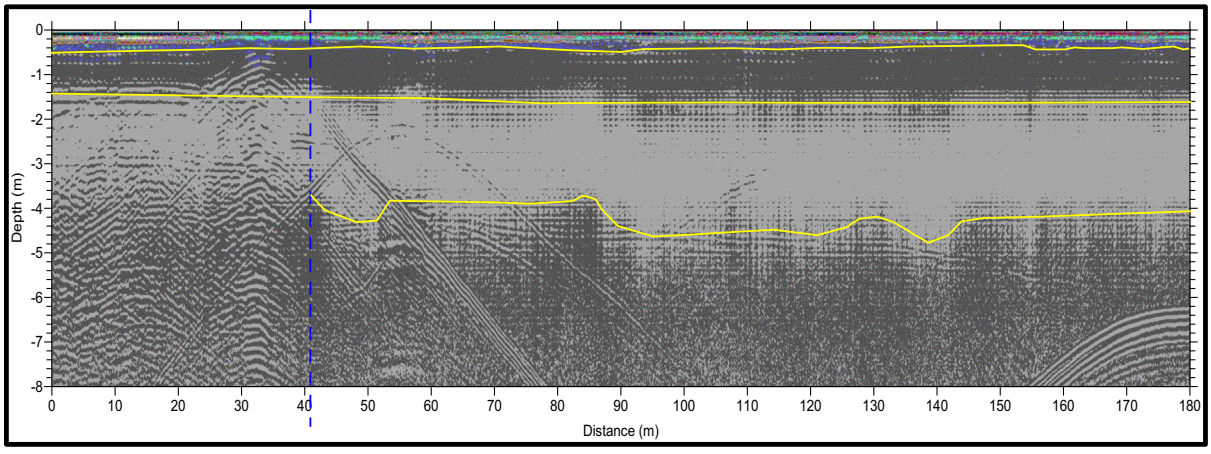

(b)

Fig. 13. (a) GPR section of the first part of profile # 7 (200 MHz antenna). (b) GPR section of the second part of profile # 7 (200 MHz antenna).

highly saturated shale deposits and of 3.6 m thick, and (4) fourth layer that extends to the end of the section (16 m) that is the echo of the third layer (multiples). It can be noted that, at the distances of 73 m and 97 m, there are two hyperbolas indicated by arrows that corresponds to sewage pipes control points.

- GPR Profile 7 (Fig. 13a and b):

This line located on the eastern side of the building and extends from south to north before, along, and after the building, with 350 m length (Fig. 5), by the 200 MHz antenna (***TW*** = 220 ns) and

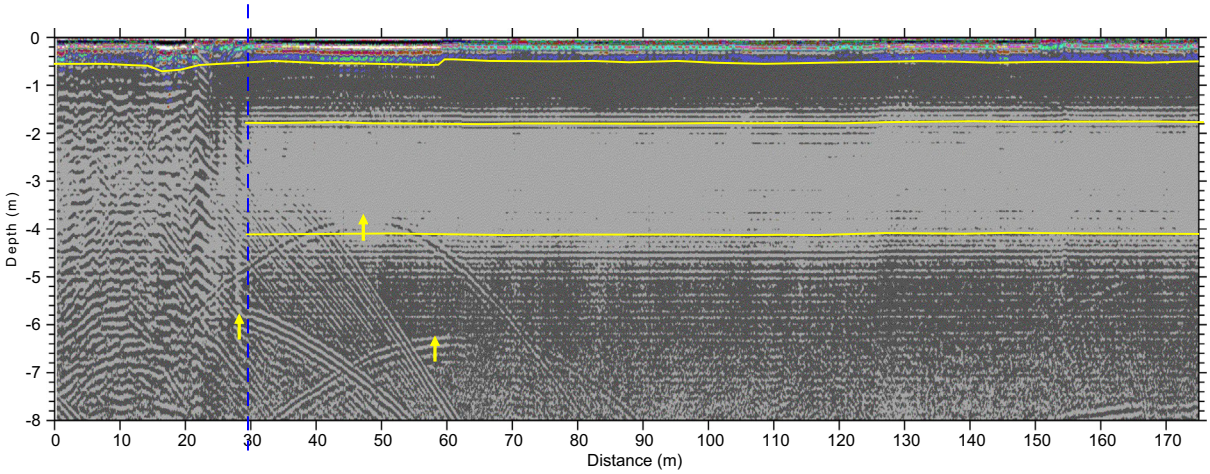

Fig. 14. GPR profile # 8 (200 MHz antenna). (The yellow arrows refer to utilities on the studied site).

applying the velocity of soil of 0.07 m/ns (the maximum depth of penetration is about 8 m). The profile (Fig. 13a and b) reveals that:

At the beginning of the profile (0–145 m) before the building:

There are four distinctive layers, (1) the first layer of a thickness of about 0.6 m which corresponds to the surface exposed layer that consists of paving and weathered materials, (2) a second layer of a thickness of about 0.9 m corresponds to saturated sand shale deposits, (3) third layer represented on the section by a strong reflector that corresponds to highly saturated shale deposits and of 2.5 m thick, and (4) fourth layer that extends to the end of the section (8 m) that is the echo of the third layer (multiples).

These layers appears again with the same order at the last 140 m of the conducted GPR profile at the distances *(210–350 m) after the building:*

At the middle part of the profile (145–210 m) along the building:

It can be noted that, the first weathered layer only is identified, but due to the high saturation, second, third, and fourth layers are masked by one highly saturated layer.

- GPR Profile 8 (Fig. 14):

This line was measured on the western part of the building, from south to north, with length 176 m (Fig. 5), by the 200 MHz antenna (***TW*** = 220 ns) and applying the velocity of soil of 0.07 m/ns (the maximum depth of penetration is about 8 m). The profile (Fig. 14) reveals that, there are four distinctive layers, (1) the first layer of a thickness of about 0.6 m which corresponds to the surface exposed layer that consists of paving and weathered materials, (2) a second layer of a thickness of about 1.5 m corresponds to saturated sand shale deposits, (3) third layer represented on the section by a strong reflector that corresponds to highly saturated shale deposits and of 2.1 m thick, and (4) fourth layer that extends to the end of the section (8 m) that is the echo of the third layer (multiples).

It can be noted that, at the beginning of the profile to the distance 30 m (length of the building) the first weathered layer only is identified, but due to the high saturation, second, third, and fourth layers are masked by one highly saturated layer. It can be noted that, there are some hyperbolas indicated by arrows that corresponds to water pipes and sewage pipes control points.

5. Discussion and conclusion

Vertical electrical sounding and GPR are practical and valuable methods to image the hydrogeological features to a depth of about 20 m in the arid shallow environment at the study area, 6th October City, Egypt. Changes in the resistivity can correlate with changes in water and moisture content as well as changes in lithology (shale content). Areas of high water content (high degree of saturation) are easily clarified at the geoelectrical resistivity results that formulated by cross-section-contoured-form and the areal distribution (contour maps). Also, the higher degree of saturations is reflected on the acquired GPR profiles through the studied site, along and around the building. So, Resistivity and GPR techniques reveal out a clear picture of saturation along/around the studied building, and verify the building zone is the zone of maximum saturation. Which, can be summarized by some factors, such as,

- Building zone is the lowest topographic zone at the whole site,
- The base of the building is lowered seven meters below the natural ground surface,
- The arbitrary irrigation for the green land that surrounds the service building may be considered to be the main source of that water rising up at the basement of the service building.
- The presence of the clay layer that acts as natural barrier for the infiltrated water coming from the surface and this water slides toward the lower surface (base of the service building).

The previously mentioned factors together, increased the water content along/around/below the studied building.

References

Annan, A.P., 1992. Ground Penetrating Radar Workshop Notes, Sensors and Softwares, Inc., Missassauga, ON, Canada, 130 pp.

Annan, A.P., Cosway, S.W., 2002. Ground Penetrating Radar Survey design. In: Proceedings of the Symposium on the Application of Geophysics to Engineering and Environmental Problmes (SAGEEP '92), Oakbrook, IL, USA, April 26–29, 2002, pp. 329–352.

Coral, Conco, 1987. Geological map of Egypt 1: 5 00 000 NH 36 NW Cairo. The Egyptian General Petroleum Corporation, Cairo, Egypt.

Davis, J.L., Annan, A.P., 1989. Ground Penetrating Radar for high resolution mapping of soil and rock stratigraphy. Geophys. Prospect. 37, 531–551.

Ghosh, D.P., 1971. The application of linear filter theory to the direct interpretation of geoelectrical resistivity sounding measurements. Geophys. Prosp. 19, 192–217.

Humphreys, G.L., Linford, J.G., West, S.M., 1990. Application of geophysics to the reclamation of saline farmland in Western Australia. Soc. Explo. Geophysics, Geotechn. Environ. Geophys., Volume II, Environ. Groundwater, pp. 175–186.

Jared, D.A., Jeffrey, E.L., 2004. Direct current resistivity profiling to study distribution of water in the unsaturated zone near the Amargosa Desert Research Site, Nevada. USGS, Open-File Report 2004-1319. U.S. Dept., of the Interior.

Johansen, H.K., 1977. A man/computer interpretation system for resistivity soundings over a horizontally stratified earth. Geophys. Prosp. 25, 667–691.

Marsden, D., 1973. The automatic fitting of a resistivity sounding by a geometrical progression of depth. Geophys. Prosp. 21, 266–280.
Mooney, H.M., Orellana, E., Pickett, H., Tornheim, L., 1966. A resistivity computation method for layered earth models. Geophys. Prosp. 31, 192–203.
Patella, D., 1975. A numerical computation procedure for the direct interpretation of geoelectrical soundings. Geophys. Prosp. 23, 335–362.
Saad, A.M., Osama, Draz M., Sakr, M., 2015. Geotechnical and Radiometric Studies for Third Manufacturing Area -6th October – Egypt, Nat. Sci. 13(5).
Stockbauer, Fred.S., Kalinec, James.A., 1995. Real-time interpretation of EM-31 and GPR data for expedited site investigation. Symp. Applicat. Geophys. Eng. Environ. Prob. 1995, 671–676.
Swartz, J.H., 1937. Resistivity studies of some salt water boundaries in the Hawaiian Islands. Trans. Am. Geophysics. Union 18, 387–393.
Szaraniec, E., 1979. Direct resistivity interpretation by accumulation of layers. Geophys. Prosp. 27, 347–362.
Tellam, J.H., Lloyd, J.W., Walters, M., 1985. The morphology of a saline groundwater body: its investigation, description and possible explanation. J. Hydrol. 83, 1–21.
Versteeg, R., 1996. Optimization of GPR acquisition and noise elimination parameters. In: Proceedings of the Sixth International Conference on Ground Penetrating Radar (GPR '96), Sendai, Japan, pp. 289–292. <http://www.sciencepub.net/nature> (pp. 33–46).